

### Acknowledgments

This manuscript was written while the first author held a National Research Council–NASA Langley research fellowship. Support from the staff and contractors of Aero Design and Development, Inc., is appreciated. Thanks also go to A. Darabi and S. Eliahu from Tel-Aviv University, and M. Livne, the former manager of the wind-tunnel center at Israel Aircraft Industries.

### References

- <sup>1</sup>Seifert, A., Darabi, A., and Wygnanski, I., "On the Delay of Airfoil Stall by Periodic Excitation," *Journal of Aircraft*, Vol. 33, No. 4, 1996, pp. 691–699.
- <sup>2</sup>Seifert, A., Bachar, T., Koss, D., Shephelovich, M., and Wygnanski, I., "Oscillatory Blowing, a Tool to Delay Boundary Layer Separation," *AIAA Journal*, Vol. 31, No. 11, 1994, pp. 2052–2060.
- <sup>3</sup>Nishri, B., and Wygnanski, I., "Effects of Periodic Excitation on Turbulent Flow Separation from a Flap," *AIAA Journal*, Vol. 36, No. 4, 1998, pp. 547–556.

## Inviscid Interactions Between Wake Vortices and Shear Layers

Z. C. Zheng\* and K. Baek†  
University of South Alabama,  
Mobile, Alabama 36688-0002

### Introduction

**A**IRCRAFT trailing vortices can be influenced significantly by atmospheric conditions such as crosswind, turbulence, and stratification. According to the NASA 1994 and 1995 field measurement program in Memphis, Tennessee,<sup>1</sup> the descending aircraft wake vortices could stall or be deflected at the top of low-level temperature inversions that usually produce pronounced shear zones.

Numerical simulations of vortex/shear interactions with ground effects have been performed by several groups.<sup>2–5</sup> Burnham<sup>6</sup> used a series of evenly spaced line vortices at a particular altitude to model the ground shear layer of the crosswind. He found that the wind shear was swept up around the downwind vortex and caused the downwind vortex to move upward, and claimed that the effect was actually produced by the vertical gradient in the wind shear rather than by the wind shear directly, because uniformly distributed wind-shear vortices would have no effect on the trailing vortex vertical motion. Recently, Proctor et al.<sup>7</sup> numerically tested the effects of narrow shear zones on the behavior of the vortex pair, motivated by the observation of the Memphis field data. The shear-layer sensitivity tests indicated that the downwind vortex was more sensitive and deflected to a higher altitude than its upwind counterpart. The downstream vortex contained vorticity of opposite sign to that of the shear. There was no detectable preference for the downwind vortex (or upwind vortex) to weaken (or strengthen) at a greater rate.

The preceding observations indicate that the mechanism responsible for the asymmetric deflection in the trailing vortices can possibly be deduced from inviscid interactions between

the vortex pair and shear layers. Based on that hypothesis, a vortex method model is developed to study that mechanism. Furthermore, this vortex method is much faster than the Navier–Stokes numerical simulations, and thus can be used for real-time predictions.

### Model Description

For the two-dimensional flow considered here, the Cauchy kernel integral for the Biot–Savart velocity can be obtained for the Lagrangian-type point vortex method used in this study.<sup>8</sup> In the current model, the primary trailing vortex pair is represented by two opposite sign point vortices. A shear layer is modeled by placing a layer of vortices, with constant circulation. Figure 1a shows an example of the initial distribution of vortices for simulating interactions between the trailing vortex pair and a narrow shear zone. The vortices in the shear layer are of the same sign as the left vortex in the vortex pair. To reduce end effects at the two ends of the shear layer,

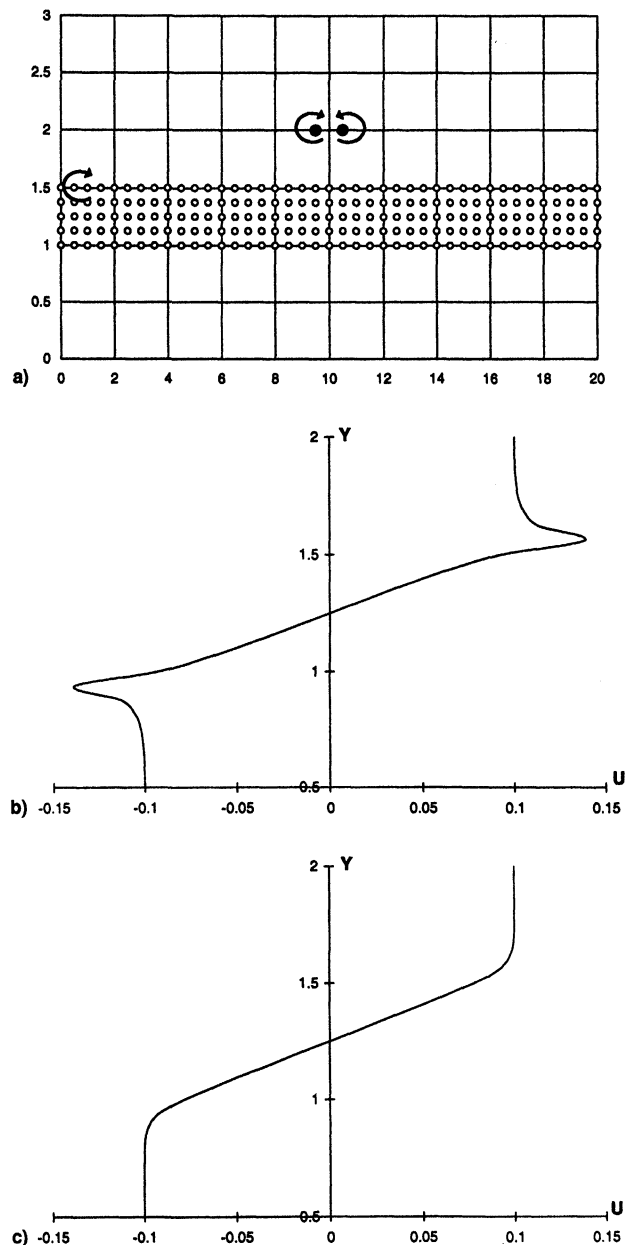


**Fig. 1** Initial flowfield: a) Vortex positions. • = the two vortices in the vortex wake, and ○ = the vortices in the shear layer. b) Velocity in  $x$  direction,  $u$ , vs height,  $y$ , at  $x$  locations aligning on the shear vortices. c) Velocity in  $x$  direction,  $u$ , vs height,  $y$ , at  $x$  locations between the shear vortices.

Received May 28, 1998; revision received Nov. 4, 1998; accepted for publication Nov. 6, 1998. Copyright © 1998 by the American Institute of Aeronautics and Astronautics, Inc. All rights reserved.

\*Assistant Professor, Mechanical Engineering Department. Member AIAA.

†Graduate Research Assistant, Mechanical Engineering Department.

periodic boundary conditions are employed in the  $x$  direction. The vortices are distributed between  $x = 0-20$  and  $y = 1-1.5$ , with 205 vortices uniformly spaced 0.5 in the  $x$  direction and 0.125 in the  $y$  direction. The periodic wavelength  $L$  in the  $x$  direction is thus chosen as 20.5. Both two-periodic series and infinite number of periodic series of images were used, with the latter showing less end effects. In the results presented in this paper, only cases with infinite number of periodic series of images are included and the solution for the flowfield becomes<sup>9</sup>

$$\frac{d\bar{z}_p}{dt} = -\frac{i}{2L} \sum_{q=1, q \neq p}^N \Gamma_q \cot \frac{\pi(z_p - z_q)}{L} \quad (1)$$

where  $z = x + iy$  and  $\bar{z}$  is the complex conjugate of  $z$ .

The computational equations have been nondimensionalized using the circulation,  $\Gamma$ , and the initial spacing,  $b$ , of the trailing vortex pair (hence, each time unit is  $b^2/\Gamma$ ). The circulation of the clockwise vortices (same sign as the left vortex) in the shear layer is represented as a certain percentage of the trailing vortex circulation. The  $u$  velocity vs height plots shown in Figs. 1b and 1c are generated by a shear layer with 2% circulation, with Fig. 1b at  $x$  locations aligning on the shear vortices and Fig. 1c between the shear vortices. It can be seen that the uniform shear is well approximated, other than a few points very close to the first layer of the shear vortices (near  $y = 1.5$  and  $y = 1$  with  $\Delta y < 0.06$ ) in Fig. 1b, because of the singularity of the point vortices. Because the singularity does not show during the simulations, that effect does not have influence on the results. The nearly constant  $u$  value away from the shear can be obtained from Eq. (1) as  $u_{unif} = n\Gamma_s/2\Delta x$ , where  $n$  is the number of rows of vortices with strength of  $\Gamma_s$  in the shear layer, and  $\Delta x$  is the  $x$ -direction spacing of the vortex row. In this case, with  $n = 5$ ,  $\Gamma_s = 0.02$ , and  $\Delta x = 0.5$ ,  $u_{unif} = 0.1$ , which is the value shown in Figs. 1b and 1c. End effects are not shown in the initial flowfield because of the periodic conditions used. Even in the later simulations with deformed shear, end effects are limited, which can be seen in Figs. 2 and 3. To test the grid size sensitivity, which is related with the number of vortices in the Lagrangian-type method used here, a shear layer with half-sized  $\Delta x$  and half of  $\Gamma_s$  has been calculated and resulted in the same velocity plots.

### Discussion of Results

Three types of flowfield setup have been considered: a shear layer below the trailing vortex pair, a shear layer above the vortex pair, and the vortex pair immersed in a constant shear. Those are the same flow types used in the shear-layer sensitivity study in Proctor et al.<sup>7</sup> It was claimed in their paper that when the shear layer had the same sign as the upwind vortex, the downwind vortex deflected higher than the upwind vortex when the shear layer was below the trailing vortex pair. When the shear layer (with the same sign of vorticity as the below one) was above the vortex pair, the upwind vortex was higher. The two vortices descended at the same rate under both no shear and constant shear environment. However, as Proctor et al. pointed out, the fluid dynamic mechanism that caused the phenomena was unclear. The following simulations are designated to understand that mechanism. It is noted that, since uniform wind does not have an effect on vortex deflection, the terminology upwind or downwind does not distinguish the behavior of the two wake vortices. The difference is the sign of each vortex in the vortex pair in comparison with the shear layer. Therefore, from now on, right and left are used instead of upwind and downwind.

Figure 2 is the time histories of vortex positions for the shear layer below vortex pair cases. The initial positions of the vortices are the same as shown in Fig. 1a, with 2% and 10% shear strengths. When the vortex pair approaches the shear layer, it deforms the shear layer gradually. It can be seen that some of the vortices in the shear layer are pushed downward as a result

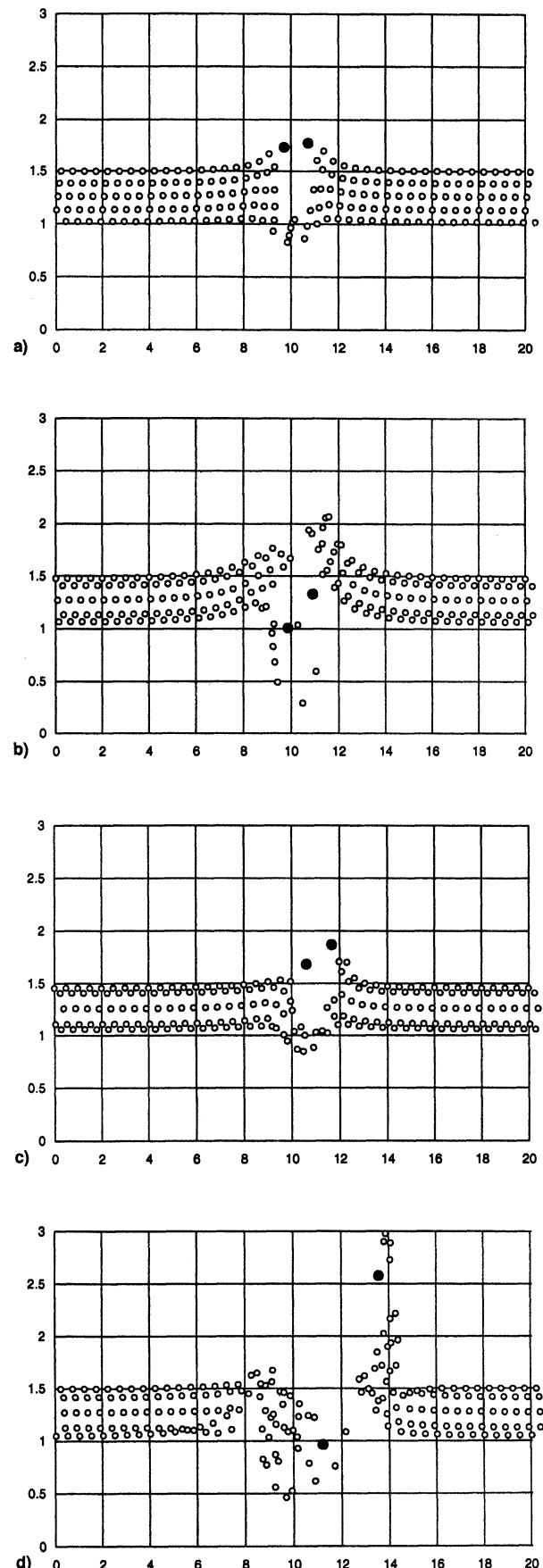


Fig. 2 Vortex position histories with shear layer below. The symbols have the same meaning as those in Fig. 1a: a) 2% shear at  $t = 1.6$ , b) 2% shear at  $t = 5.6$ , c) 10% shear at  $t = 1.6$ , and d) 10% shear at  $t = 5.6$ .

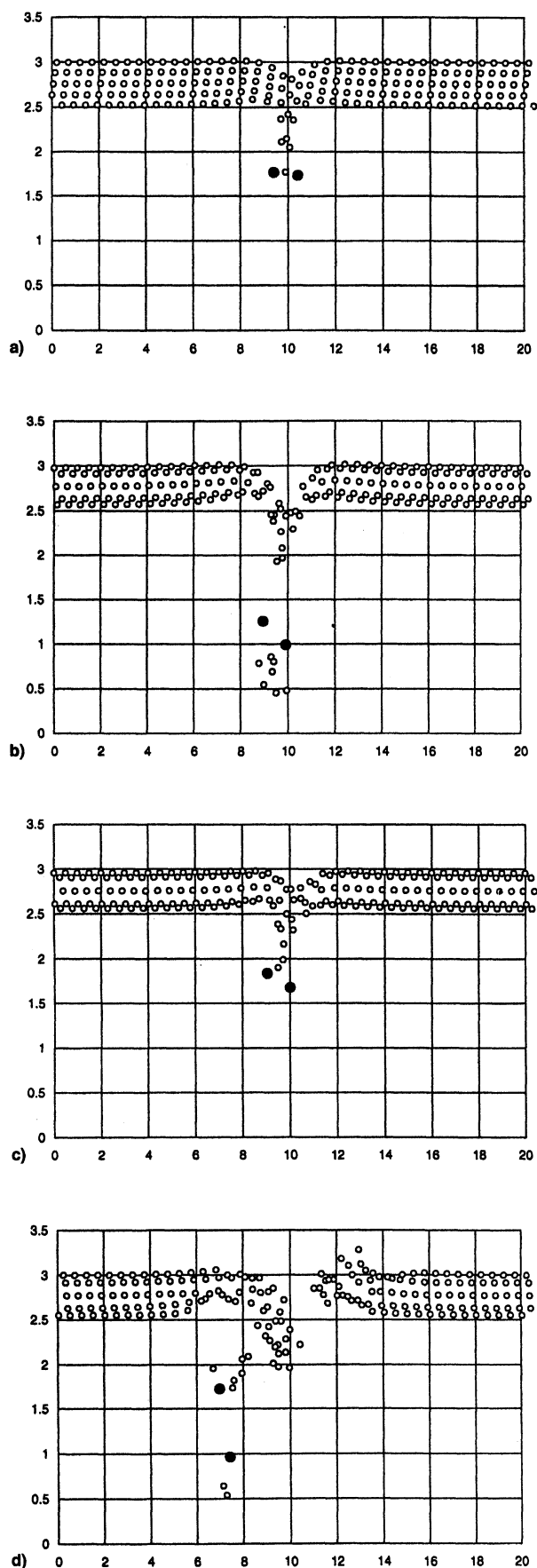


Fig. 3 Vortex position histories with shear layer above. The symbols have the same meaning as those in Fig. 1a: a) 2% shear at  $t = 1.6$ , b) 2% shear at  $t = 5.6$ , c) 10% shear at  $t = 1.6$ , and d) 10% shear at  $t = 5.6$ .

of the induced downwash by the vortex pair, some are lifted and wrapped around the vortex pair when the vortex pair is close to the shear layer. Note that the vortices in the shear layer are in the same sense as the left vortex and in the opposite sense of the right vortex of the wake vortex pair. The opposite sign vortices near the right vortex tend to reduce the vertical motion of the right vortex, similar to the mechanism of vortex rebound near the ground, which is a result of the induced opposite sign secondary vortices from the ground boundary.<sup>10</sup> Therefore, after some time of interactions, the right vortex descends less than the left vortex for the weak shear case (2%), whereas for the strong shear case (10%) the right vortex stops descending and deflects from the shear layer.

The same 2% and 10% shear layers are then placed above the vortex pair. The vortex position histories are shown in Fig. 3. At  $t = 1.6$ , the vortices in the shear layer are pulled in between the vortex pair, because of the shape of streamlines around the vortex pair. Because the vortices from the shear layer are in the middle of the vortex pair, they produce the opposite effects to those in Fig. 2. The clockwise shear vortices are now on the right side of the left vortex and on the left side of the right vortex. Hence, they induce upward motion on the left vortex and downward motion on the right vortex, and eventually cause the right vortex to descend more than the left vortex.

Trajectories of the trailing vortex pair are plotted in Fig. 4 for three shear-strength levels (2, 4, and 10%), for both shear-below and shear-above cases. It shows that when the shear-layer strength is increased, the altitude difference in left and right vortices is increased. It is noted that for the intermediate strength shear layer (4%), the right vortex almost stays at the same position or stalls at the later time levels.

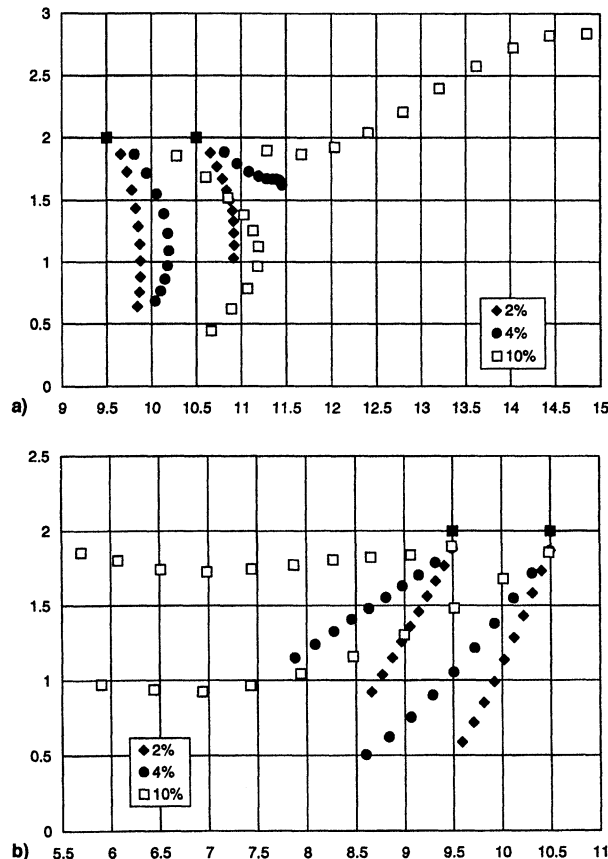


Fig. 4 Trajectories of the vortex pair under different shear strengths, with a) shear layer below and b) above. The time between each symbol interval is a 0.8 dimensionless time unit. The total time is 8 dimensionless time units.

Under the constant shear environment, i.e., when the shear layer is not a concentrated zone but a large region with constant shear around the vortex pair, Brashears et al.<sup>11</sup> showed, using an inviscid method, that there was no influence on the vortex descent behavior. We made a test to allow the vortex pair to pass through a nondeformed shear layer by fixing the shear vortex positions during the simulations. The nondeformed shear layer approximated a constant shear when the vortex pair penetrated the shear layer. That test did not show altitude differences between the two vortices.

### Conclusions

It has been shown, from the inviscid vortex method simulations, that the shear-layer deformation causes the vortex descent history difference in the two vortices of the trailing vortex pair. Because of the interactions between the vortices from the shear layer and the vortex pair, the induced velocities on the vortex pair have been changed. Such changes produce different trajectories when the vortex pair is interacting with a concentrated shear layer below or above it. The results show that if a shear layer is put below the vortex pair containing shear vortices with the same sign as the left vortex, the right vortex descends less than the left vortex. While the same shear layer is set above the vortex pair, the right vortex descends more. The descent altitude difference increases with the shear-layer strength. The two vortices of the trailing vortex pair do not show altitude difference when they go through a constant, nondeformed shear layer. These trends are the same as predicted by Proctor et al.<sup>7</sup> in their finite difference numerical simulations using the Navier–Stokes equations. Modifications of this model to include other atmospheric conditions are feasible for real-time wake vortex predictions.

### Acknowledgments

This research was done under the support of NASA research Grant NAG1-1911 from the NASA Langley Research Center. F. H. Proctor was the Technical Monitor. The authors would like to thank S. H. Lim for help with revising most of the figures.

### References

- Mathews, M. P., Dasey, T. J., Perras, G. H., and Campbell, S. D., "Planetary Boundary Layer Measurements for the Understanding of Aircraft Wake Vortex Behavior," 7th Conf. on Aviation Weather Systems, Long Beach, CA, American Meteorology Society, Paper 5-5, 1997.
- Bilanin, A. J., Teske, M. E., and Hirsh, J. E., "Neutral Atmospheric Effects on the Dissipation of Aircraft Vortex Wakes," *AIAA Journal*, Vol. 16, No. 9, 1978, pp. 956–961.
- Liu, C. H., and Ting, L., "Interaction of Decaying Trailing Vortices in Spanwise Shear Flow," *Computers and Fluids*, Vol. 15, No. 1, 1987, pp. 77–92.
- Robins, R. E., and Delisi, D. P., "Potential Hazard of Aircraft Wake Vortices in Ground Effect with Crosswind," *Journal of Aircraft*, Vol. 30, No. 2, 1993, pp. 201–206.
- Zheng, Z. C., Ash, R. L., and Greene, G. C., "A Study of the Influence of Cross Flow on the Behavior of Aircraft Wake Vortices near the Ground," *Proceedings of the 19th Congress of the International Council on the Aeronautical Sciences*, Vol. 2, AIAA, Washington, DC, 1994, pp. 1649–1659.
- Burnham, D. C., "Effect of Ground Wind Shear on Aircraft Trailing Vortices," *AIAA Journal*, Vol. 10, No. 8, 1972, pp. 1114, 1115.
- Proctor, F. H., Hinton, D. A., Han, J., Schowalter, D. G., and Lin, Y. L., "Two Dimensional Wake Vortex Simulations in the Atmosphere: Preliminary Sensitivity Studies," AIAA Paper 97-0056, Jan. 1997.
- Leonard, A., "Vortex Methods for Flow Simulation," *Journal of Computational Physics*, Vol. 37, 1980, pp. 289–335.
- Lamb, H., *Hydrodynamics*, 6th ed., Dover, New York, 1945.
- Zheng, Z. C., and Ash, R. L., "A Study of Aircraft Wake Vortex Behavior Near the Ground," *AIAA Journal*, Vol. 34, No. 3, 1996, pp. 580–589.
- Brashears, M. R., Logan, N. A., and Hallock, J. N., "Effect of Wind Shear and Ground Plane on Aircraft Wake Vortices," *Journal of Aircraft*, Vol. 12, No. 10, 1975, pp. 830–833.

## Model for Development of Backlash in Aircraft Control Circuit Mechanical Links

S. A. Safi,\* D. W. Kelly,† and R. D. Archer‡  
University of New South Wales,  
Sydney, Wales 2052, Australia

### Nomenclature

- $b$  = semichord length
- $C$  = Theodorsen's function
- $d$  = inside diameter of the bearing
- $h$  = plunging displacement
- $I_B$  = mass moment of inertia of the aileron about aileron hinge line
- $k$  = specific wear rate coefficient
- $k_h$  = bending stiffness of the wing
- $k_\beta$  = torsional stiffness of the aileron
- $M$  = restoring moment, Eq. (2)
- $m$  = mass of wing–aileron segment (per unit span)
- $N$  = frequency of oscillation equal to the frequency of limit cycle oscillation of the aileron
- $P$  = nominal pressure
- $S_\beta$  = static mass moment of aileron about aileron hinge line
- $T_i$  = geometric functions given in Ref. 5
- $t$  = time
- $U$  = airspeed
- $V$  = rubbing speed
- $V_f$  = flutter velocity of the linear system
- $w$  = depth of wear
- $\beta$  = control surface rotation
- $\beta_0$  = amount of freeplay
- $\theta$  = angle between limits of rotation
- $\rho$  = air density

### Introduction

THE assumption of structural linearity has usually been made when determining the flutter characteristics of aircraft structures. However, aircraft structures often exhibit nonlinearities that can have a significant effect on the flutter speed and aeroelastic response. For example, it is known that airfoils and wing–aileron systems with structural nonlinearity sometimes demonstrate limit cycle oscillation (LCO) below the flutter boundary of the linear system. It is also known that aging has a significant effect on developing concentrated nonlinearity in mechanical systems. One particular example is worn control surface hinges that lead to a freeplay nonlinearity, called backlash. Nonlinear systems experiencing LCO are likely to require maintenance because of accelerated fatigue and wear.

Woolston et al.<sup>1</sup> studied the effects of several types of structural nonlinearities on wing and control surface flutter. The results for the nonlinear wing and control surface showed the existence of sustained oscillation of limited amplitude below the flutter speed of the linear system for a particular case.

In recent years, the modeling and analysis of aerosurfaces with structural nonlinearities has been the subject of numerous investigations. Yang and Zhao<sup>2</sup> performed experimental and theoretical analysis to investigate oscillations of a two-degree-of-freedom wing model with nonlinear pitching stiffness. They made a comprehensive study of LCO of the two-degree-of-freedom model subjected to incompressible flow using the

Received May 17, 1998; revision received Aug. 12, 1998; accepted for publication Aug. 24, 1998. Copyright © 1998 by the American Institute of Aeronautics and Astronautics, Inc. All rights reserved.

\*Graduate Student, Department of Aerospace Engineering.

†Associate Professor, Department of Aerospace Engineering.